

A model equation for axisymmetric stability of small-gap parallel-plate flows.

Yuriko Renardy and Michael Renardy
Department of Mathematics and ICAM
Virginia Polytechnic Institute and State University
Blacksburg, VA 24061-0123, U.S.A.

October 29, 1997

Abstract

We consider a model equation derived in [18] for the linear stability of a torsional flow of an Oldroyd-B fluid in a parallel-plate device. Axisymmetry, small gap and zero Reynolds numbers are assumed. The equation is not separable in the radial and vertical variables. The advantage is that its eigenmodes depend only on the aspect ratio. Once evaluated, the eigenmodes are used to calculate the onset conditions for any retardation parameter and Deborah number. The onset conditions and streamfunction contours are compared with the normal-mode analysis of [14] which assumed radially localized disturbances, and the computational results on the full equations [1]. Two facets of the model equation are discussed; first, how well the onset conditions and eigenmodes compare with those of the case where the radially localized assumption is made, and secondly, how they approximate those of the full equations.

1 Introduction

Rotational flows of a viscoelastic fluid in parallel-plate and cone-and-plate geometries undergo an elastic instability as the Deborah number is increased past a critical value [21]; this is of importance in understanding the flow in rheometric devices [23]. Observations and stability analyses for radially localized modes and non-axisymmetric modes are discussed in [3, 9, 10, 20], and the effect of inertia is discussed in [22]. Asymptotic analyses for small gap are given in [11, 12, 13, 14, 15, 16, 17, 18], and show that for zero Reynolds number and axisymmetry, stability is controlled by a local elasticity number \mathcal{E} . For \mathcal{E} less than a critical value, the flow is linearly stable. As \mathcal{E} increases past the critical value, the flow loses stability to a time dependent oscillatory mode. Assuming short-wave radially localized solutions, the linear stability problem for parallel plates is solved analytically in [20, 14, 18]. The assumption of radial confinement leads to a normal mode analysis where separable solutions

are found, on the basis that the disturbance would be short-wave and die out away from a critical radius. The eigensolution would be localized toward the outer edge of the device. The assumption of radial localization is necessary in the parallel plate problem in order to obtain a problem which can be separated and reduced to one space dimension. In the cone-and-plate geometry, in contrast, the problem is always separable as long as the extent of the cone and plate is presumed infinite. Nonseparability, however, arises in this geometry as well if the outer boundary of the device is taken into account. It turns out that, with the approximation of localized disturbances, the parallel-plate problem leads to exactly the same eigenvalue relation as the cone-and-plate problem (as long as small gap is assumed), see [14, 18]. The equation discussed in this paper also has an analogue in the cone-and-plate problem, but the equations are not identical, since analogous terms involve different powers of the radius.

In this note, we address the question of what the solutions for the parallel-plate problem are if the radial confinement assumption is not made. Under these conditions, the equation is still simple, and it would be of interest to see what the solutions would be, and separately, how they agree with the full numerical solutions of [1] which do not assume small gap or radially localized modes. The latter work includes a boundary at $r = 1$. It is shown that as the aspect ratio decreases, a number of roll cells appear. The amplitude of the roll cells near the center is much smaller in magnitude than the amplitude of the roll cells near the outer boundary. It is also found that there is an almost linear relationship between the aspect ratio and the critical Deborah number at small values of the aspect ratio. We show below that the simple model equation derived by Olagunju captures many features of the full solutions when used for small gaps. An advantage of the model equation is that its eigensolutions depend only on the aspect ratio. Once these are found, we can determine the growth rates for any Deborah number and retardation parameter as exact solutions of a quartic equation. Moreover, we can find the critical Deborah number by solving a sixth degree equation.

2 The Model Equation

We adopt the notation of [18] for flow of an Oldroyd-B fluid confined between two parallel coaxial disks, gap height h , radius a . The top plate rotates with angular speed ϖ and the bottom plate is stationary. Cylindrical coordinates (r, θ, z) are used. We denote by λ the relaxation time, η_s and η_p are the solvent and polymer viscosities, $\dot{\gamma} = \varpi/a$ is a shear rate. The problem is nondimensionalized as follows: $\tilde{r} = r$, $\tilde{t} = \dot{\gamma}t$, $\tilde{z} = hz$, $\tilde{\mathbf{v}} = a\varpi\mathbf{v}$. The dimensionless parameters are the aspect ratio $\alpha = a/h$, the retardation parameter $\beta = \eta_p/(\eta_s + \eta_p)$, $De = \lambda\varpi$, $We = De/\alpha$, $\tilde{De} = rDe$. In summary, disturbances which are valid to leading order as $\alpha \rightarrow 0$ are kept in the asymptotic derivation, the radial variable is rescaled to ρ where $0 < \rho < 1/\alpha$, and streamfunction solutions of the form $\chi = \exp(\omega t)\chi'$ are sought. The problem is shown to reduce to a single equation, Eq. (39) of [18]:

$$\nabla^4 \chi' + \Lambda \frac{\partial^3 \chi'}{\partial \rho \partial^2 z} = 0. \quad (1)$$

Here we have

$$\nabla^2 = \frac{\partial^2}{\partial \rho^2} + \frac{1}{\rho} \frac{\partial}{\partial \rho} + \frac{\partial^2}{\partial z^2}.$$

The term $\frac{1}{\rho} \frac{\partial}{\partial \rho}$ is actually of lower order in Olagunju's shortwave analysis, but by including it we avoid the need for imposing a boundary condition at $\rho = 0$. It is clear that the inclusion or noninclusion of this term alters the behavior near $\rho = 0$, but in any case the validity of the short wave approximation breaks down if ρ is small, and hence the solution near $\rho = 0$ cannot be expected to have physical relevance. The boundary conditions are

$$\chi' = \frac{\partial \chi'}{\partial z} = 0 \quad \text{at} \quad z = 0, 1, \quad (2)$$

$$\chi' = \frac{\partial^2 \chi'}{\partial \rho^2} = 0 \quad \text{at} \quad \rho = 1/\alpha. \quad (3)$$

The boundary conditions at $\rho = 1/\alpha$ correspond to zero radial velocity and zero shear rate (and hence zero shear stress).

From Eq. (38) of [18], it is evident that $\Lambda = \lambda\rho$, where the eigenvalue λ is a constant. After multiplying through by ρ^3 , the equation becomes

$$\begin{aligned} \rho^3 \chi'_{zzzz} + \chi'_\rho + 2\rho^2 \chi'_{\rho zz} - \rho \chi'_{\rho\rho} + 2\rho^3 \chi'_{\rho\rho zz} \\ + 2\rho^2 \chi'_{\rho\rho\rho} + \rho^3 \chi'_{\rho\rho\rho\rho} = -\lambda\rho^4 \chi'_{\rho zz}. \end{aligned} \quad (4)$$

For each aspect ratio α , the eigenmodes χ' and eigenvalues λ of Eq.(4) are evaluated. Once these are available, then the original eigenvalues ω can be calculated for any given retardation parameter β and De by using Eq. (38) of [18] (or Eq.(4.20) of [14]). With $\mathcal{E} = \tilde{\text{De}}We$, $\tilde{\text{De}} = \rho\alpha\text{De}$, this yields a quartic equation for $\Omega = \omega We$:

$$\begin{aligned} (\lambda - 2\beta\lambda + \beta^2\lambda)\Omega^4 + (4\lambda - 6\beta\lambda + 2\beta^2\lambda)\Omega^3 \\ + (6\lambda - 6\beta\lambda + \beta^2\lambda - 2\alpha\beta\text{De}We + 2\alpha\beta^2\text{De}We)\Omega^2 \\ + (4\lambda - 2\beta\lambda - 8\alpha\beta\text{De}We + 8\alpha\beta^2\text{De}We)\Omega + \lambda - 6\alpha\beta\text{De}We + 4\alpha\beta^2\text{De}We = 0. \end{aligned} \quad (5)$$

This quartic is solved using radicals; a description of the algorithm for this can be found in [7], pp. 237-238.

2.1 Asymptotic analysis for large DeWe

Consider the quartic equation (5) large values of DeWe. Then two of the Ω s are given by the quadratic equation that results from retaining terms of order DeWe:

$$(-2\alpha\beta + 2\alpha\beta^2)\Omega^2 + (-8\alpha\beta + 8\alpha\beta^2)\Omega - 6\alpha\beta + 4\alpha\beta^2 = 0.$$

This simplifies to

$$(\Omega + 2)^2 + \frac{1 - 2\beta}{\beta - 1} = 0.$$

These eigenvalues are always stable. The other two eigenvalues are proportional to \sqrt{DeWe} , and to leading order, they are given by

$$(\lambda - 2\beta\lambda + \beta^2\lambda)\Omega^2 + (2\alpha\beta^2 - 2\alpha\beta)DeWe = 0,$$

or

$$\lambda(1 - \beta)\Omega^2 - 2\alpha\beta DeWe = 0.$$

One of these will always be unstable unless λ is real and negative.

The above applies to $0 < \beta < 1$. If $\beta = 1$, then a number of terms in the quartic cancel, and the remaining equation is

$$\lambda\Omega^2 + 2\lambda\Omega + \lambda - 2\alpha DeWe = 0,$$

i.e.

$$(\Omega + 1)^2 = \frac{2\alpha DeWe}{\lambda}.$$

Again this leads to instability for large $DeWe$, unless λ is real and negative.

3 Eigenmodes of the model equation

We express the solution in a double Chebyshev expansion, transforming to new variables

$$\rho = \frac{1}{2\alpha}(\rho' + 1), \quad -1 < \rho' < 1, \quad \text{and} \quad z' = 2z - 1, \quad -1 < z' < 1,$$

$$\chi' = \sum_{j=0}^N \sum_{m=0}^M b_{jm} T_m(\rho') T_j(z').$$

From this, a matrix equation $AX = \lambda BX$ for $X = b_{jm}$ is constructed. This method yields some inaccurate wiggles at $\rho = 0$. These can be avoided if instead, we set $\rho = \rho'/\alpha$ and use only Chebyshev polynomials even in ρ' in the solution. However, both schemes produce the same results very quickly away from the centerline. Comments on these points are found in [5]. Figure 1 shows the temporal eigenvalues ω retrieved by substitution of the λ into the quartic equation (5) at $\beta = 0.41, \alpha = 0.1, De=2$, excluding numerous ones which are not involved in instabilities. The onset modes are shown. Once the λ corresponding to the onset eigenvalues ω is found, then the algorithm of the following section determines the onset conditions exactly. Hence, it is not necessary to compute results such as those of Figure 1 more than once for each aspect ratio.

Table 1 shows the eigenvalues against the aspect ratio.

The streamfunction is a function of ρ, z and time, and the onset mode oscillates, taking on the values $\text{Re}\chi'$ and $\text{Im}\chi'$ during the cycle. Analogously to the figures of [1], we show the contours of these two quantities. Figure 2 shows the trends as the aspect ratio decreases. For aspect ratio $\alpha = 0.1$, [1] find 9 roll cells in the real part of the streamfunction and 10 in the imaginary part. Figure 2 (c-d) show agreement with this, and in more detail, specific contour values for $\alpha = 0.1$ are shown in Figure 3. The qualitative features of the modes for larger aspect ratios are also similar, though these are expected to diminish since the model

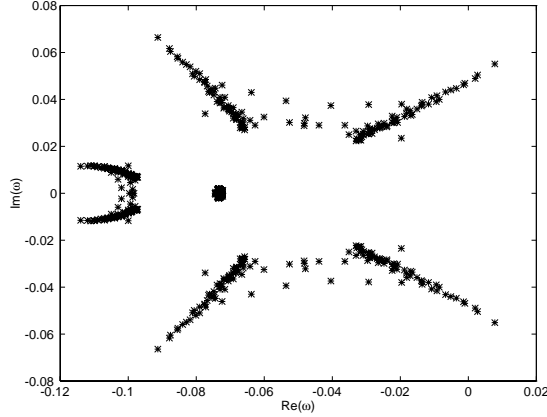


Figure 1: The least stable eigenvalues ω are shown at $\beta = 0.41, \alpha = 0.1, De=2$. This excludes numerous ones which are located in the center of the figure and are not involved in instabilities.

equation was derived under the assumption of small aspect ratios. The contours for the case $\alpha = 0.75, 1.0$ are shown in Figure 4 for comparison with those of [1]. The contour plots for $\alpha \geq 0.5$ show features which are different from those of [1] due to mode cross-overs. The second most unstable mode for $\alpha = 0.5$ at $\lambda = -5.15 \pm 20.85i$ produces the streamfunction shown in Figure 5, which has similarities with the mode for smaller α . Moreover, the second most unstable mode at $\alpha = 1$ is shown in Figure 6, and this has the appearance of the mode captured by [1].

4 Onset conditions

To evaluate neutral stability conditions for a given β and De , set $\Omega = i\nu$ in the quartic equation (5), and separate out the real and imaginary parts of the equation. We denote these functions by $p1[\nu, w]$ and $p2[\nu, w]$, w is the combination $\alpha De We$. We use Mathematica and provide the input file in Appendix A. The command `Resultant [p1 [nu, w], p2[nu, w], nu]` determines the condition that $p1$ and $p2$ have a common root ν . This yields a sixth degree polynomial in w . We then input numerical values for λ and β and find the roots of the sixth degree polynomial. The positive root gives the stability threshold for $\alpha De We = De^2$. This algorithm can be used to find the stability threshold for any λ . For aspect ratio $\alpha = 0.1$, Figure 7 shows the critical $\alpha De We$ vs β . Since $\alpha De We = De^2$, we calculate De vs. β from this as shown in Figure 8. For the cone-and-plate geometry, Figure 1 of [14] shows neutral stability curves against \mathcal{E} for $\beta = 0.1, 0.25, 0.75, 1.0$. The minimum is attained at $\beta = 1, 0.5$, as in Fig.8. The numerical value of \mathcal{E} is approximately 22, and $\mathcal{E} = De^2/\alpha$, so that a comparison with Figure 8 at $\alpha = 0.1$ yields similar results. Figure 9 shows the linear trend in the relationship between the critical Deborah number and aspect ratio α at fixed $\beta = 0.41$, and this compares well with Figure 7 of [1].

Table 1: The eigenvalues λ of Eq.(4) that yield onset modes

α	λ
0.05	$-0.026 \pm 1.224i$
0.1	$-0.101 \pm 2.670i$
0.2	$-0.504 \pm 6.134i$
0.25	$-0.865 \pm 8.14i$
0.3	$-1.36 \pm 10.33i$
0.5	$-3.325 \pm 23.544i$
0.75	$-9.64 \pm 41.04i$
0.9	$-16.02 \pm 53.23i$
1.0	$-21.724 \pm 61.969i$

5 Conclusions

We have investigated the stability of Oldroyd-B flow in the parallel plate rheometer using a simplified theory based on small gap, but without the assumption of radially localized solutions. The resulting partial differential equation is not separable. Nevertheless, there is significant simplification. The essential part of the solution involves an eigenvalue problem which depends only on the aspect ratio, and not at all on the Weissenberg number and retardation parameter. Once this eigenvalue problem is solved, the growth rates and onset conditions can be determined by solving polynomial equations. The results are in good qualitative agreement with full numerical simulations.

Acknowledgment

This work is funded by ONR N00014-92-J-1664, NSF-CTS 9612308 and NSF-DMS 9622735. We thank David Olagunju for suggesting this problem.

References

- [1] Avagliano, A. and Phan-Thien, N. 1996 Torsional flow: elastic instability in a finite domain, *J. Fluid Mech.* **312**, 279-298.
- [2] Bird, R. B., Armstrong, R. C., and Hassager, O. 1987 *Dynamics of Polymeric Liquids*, Vol. 1, second edition, John Wiley & Sons, New York.
- [3] Byars, J. A., Oztekin, A., Brown, R. A. & Mckinley, G. H. 1994 Spiral instabilities in the flow of highly elastic fluids between rotating parallel disks, *J. Fluid Mech.* **271**, 173-218.
- [4] Crewthers, I., Huilgol, R. R. and Josza, R. J. 1991 Axisymmetric and nonaxisymmetric flows of a non-Newtonian fluid between coaxial rotating discs, *Phil. Trans. Roy. Soc. London A* **337**, 467-495.
- [5] Gottlieb, D., and Orszag, S. A., 1977 Numerical analysis of spectral methods: theory and applications, CBMS-NSF Regional Conference Series in Applied Mathematics, SIAM, Philadelphia, PA.
- [6] Heuser, G, and Krause, E. 1979 The flow field of Newtonian fluid in cone and plate viscometers with small gap angles, *Rheol. Acta* **18**, 553-564.
- [7] Hornfeck, B. 1976 *Algebra*, 3rd ed., De Gruyter, Berlin.
- [8] Magda, J. J., and Larson, R. G. 1988 A transition occurring in ideal elastic liquids during shear flows. *J. Non-Newton. Fluid Mech.* **30**, 1-19.
- [9] McKinley, G. H., Byars, J. A., Brown, R. A., and Armstrong, R. C. 1991 Observations on the inelastic instability in cone-and-plate flow of a polyisobutylene Boger fluid, *J. Non-Newton. Fluid Mech.* **40**, 201.
- [10] McKinley, G. H., Oztekin, A., Byars, J. A., and Brown R. A. 1995 Self-similar spiral instabilities in elastic flows between a cone and a plate, *J. Fluid Mech.* **285**, 123.
- [11] Olagunju, D. O. 1993 Asymptotic analysis of the finite cone-and-plate flow of a non-Newtonian fluid, *J. Non-Newton. Fluid Mech.* **50**, 289-303.
- [12] Olagunju, D. O., and Cook, L. P. 1993 Linear stability analysis of cone and plate flow of an Oldroyd-B fluid. *J. Non-Newton. Fluid Mech.* **47**, 93-105.

- [13] Olagunju, D. O. 1995a Instabilities and bifurcations of von-Kármán similarity solutions in swirling viscoelastic flow. *J. Appl. Math. Phys. (ZAMP)* **46**, 224–238.
- [14] Olagunju, D. O. 1995b Elastic instabilities in cone-and-plate flow: Small gap theory. *J. Appl. Math. Phys. (ZAMP)* **46**, 946–959.
- [15] Olagunju, D. O. 1996a Hopf bifurcation in creeping cone-and-plate flow of a viscoelastic fluid. to appear *J. Appl. Math. Phys. (ZAMP)*.
- [16] Olagunju, D. O. 1996b Analytical results on stability of cone-and-plate flow for $Re \neq 0$. *XIIIth Int. Cong. Rheol.* Quebec. Canada.
- [17] Olagunju, D. O. 1997a Inertial effect on stability of cone-and-plate flow, to appear *J. Fluid Mech.*
- [18] Olagunju, D. O. 1997b On short wave elastic instabilities in parallel plate flow, Proceedings of the ASME Annual Meeting.
- [19] Orszag, S. A. 1971 Accurate solutions of the Orr-Sommerfeld stability equation, *J. Fluid Mech.* **50**, 689.
- [20] Oztekin A, and Brown, R. A. 1993 Instability of a viscoelastic fluid between rotating parallel disks: analysis for the Oldroyd-B fluid. *J. Fluid Mech.* **225**, 473–502.
- [21] Phan-Thien, N. 1983 Coaxial-disk flow of an Oldroyd-B fluid: exact solution and stability, *J. Non-Newt. Fluid Mech.* **13**, 325-340.
- [22] Renardy, Y. and Olagunju, D.O. 1997 Inertial effect on stability of cone-and-plate flow. Part 2: Non-axisymmetric modes, submitted to *J. Non-Newt. Fluid Mech.*
- [23] Walters, K. and Waters, N. D. 1968 On the use of rheogoniometers, Part I – Steady Shear, Polymer Systems, Macmillan, 211-235.

Appendix A: Stability threshold

The following Mathematica file evaluates the stability threshold of Eq. (5). The real and imaginary parts of λ are denoted by lam1 and lam2, respectively. The value of β needs to be inputted after the Resultant command. The result w denotes the critical α DeWe and is written into the file 'solvew'.

```
p1[nu_,w_]=lam1*(1-beta)^2*nu^4+lam2*(4-6beta+2beta^2)*nu^3
p1[nu_,w_]=p1[nu,w]-lam1*(6-6beta+beta^2)*nu^2+2*w*beta*(1-beta)*nu^2
p1[nu_,w_]=p1[nu,w]-lam2*(4-2beta)*nu+lam1-6beta*w+4beta^2w
p2[nu_,w_]=lam2*(1-beta)^2*nu^4-lam1*(4-6beta+2beta^2)*nu^3
p2[nu_,w_]=p2[nu,w]-lam2*(6-6beta+beta^2)*nu^2+w*(-8beta+8beta^2)*nu
p2[nu_,w_]=p2[nu,w]+lam1*(4-2beta)*nu+lam2
q[w]=Resultant[p1[nu,w],p2[nu,w],nu]
lambdas=OpenRead["lambdas.dat"]
lam1=Read[lambdas,Number]
lam2=Read[lambdas,Number]
Close[lambdas]
beta=0.75
f1=Solve[q[w]==0,w]
Put[f1,"solvew"]
```

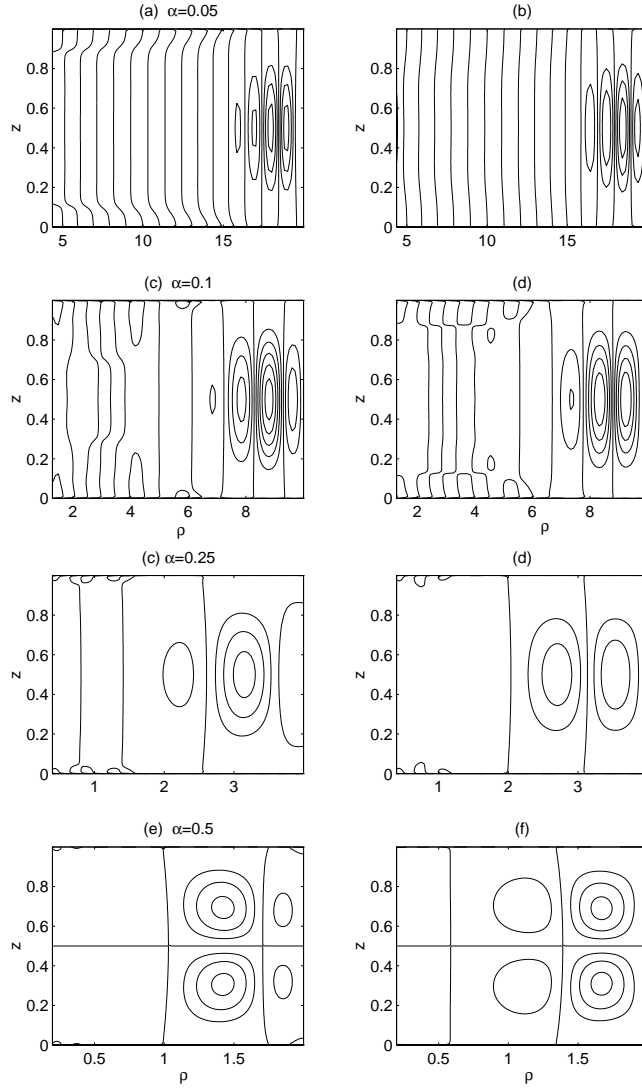


Figure 2: Contours of the disturbance streamfunction χ' for aspect ratios $\alpha = 0.1, 0.05, 0.25, 0.5$. (a), (c), (e) and (g) are $\text{Re}\chi'$; (b), (d), (f) and (h) are $\text{Im}\chi'$.

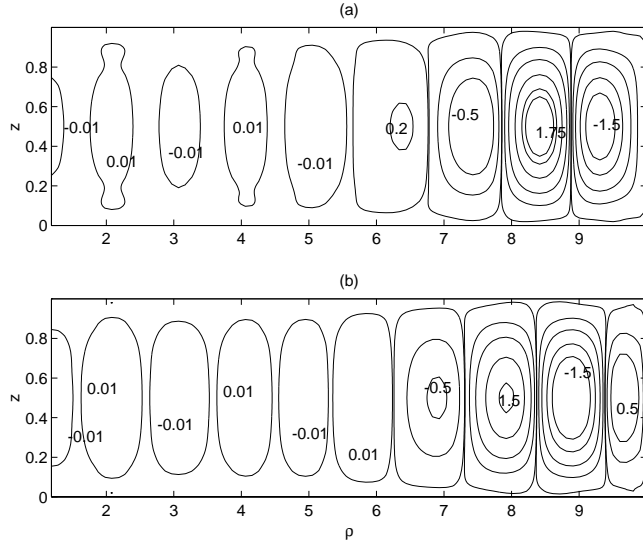


Figure 3: Contours of the disturbance streamfunction χ' for aspect ratio $\alpha = 0.1$ with some contour values (a) $\text{Re}\chi'$, (b) $\text{Im}\chi'$.

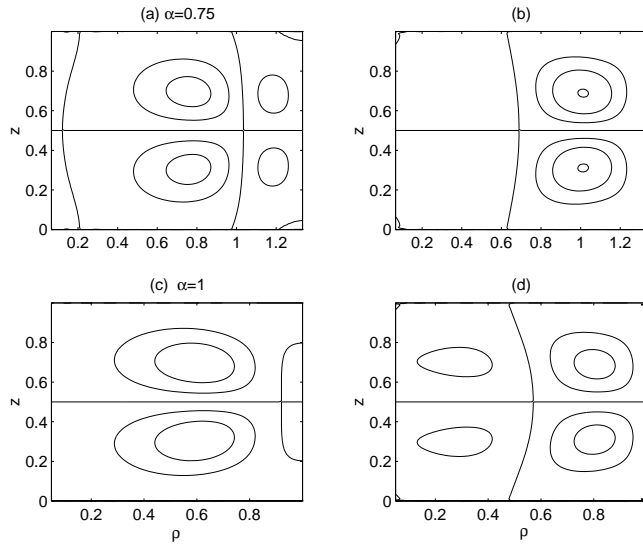


Figure 4: Contours of the disturbance streamfunction χ' for aspect ratios $\alpha = 0.75, 1.0$. (a) and (c) are $\text{Re}\chi'$, (b) and (d) are $\text{Im}\chi'$.

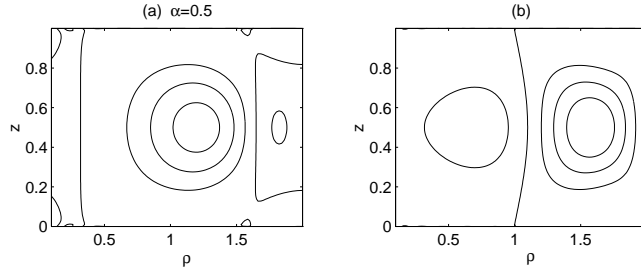


Figure 5: Contours of the disturbance streamfunction χ' for $\lambda = -5.15 \pm 20.85i$, aspect ratios $\alpha = 0.5$. (a) $\text{Re}\chi'$, (b) $\text{Im}\chi'$.

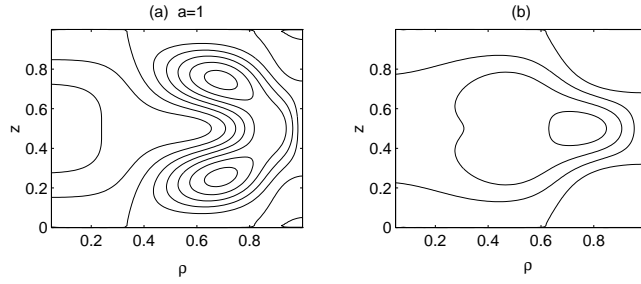


Figure 6: Contours of the disturbance streamfunction χ' for the second unstable mode $\lambda = -19.9 - 72.27i$, aspect ratios $\alpha = 1$. (a) $\text{Re}\chi'$, (b) $\text{Im}\chi'$.

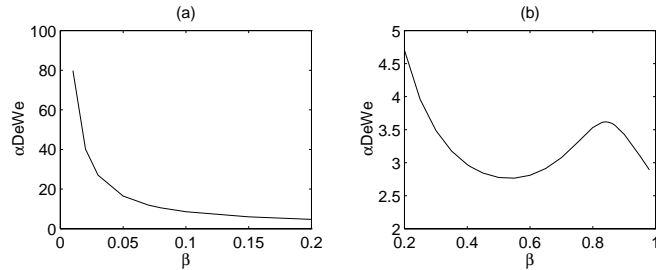


Figure 7: The critical αDeWe vs β for aspect ratio $\alpha = 0.1$.

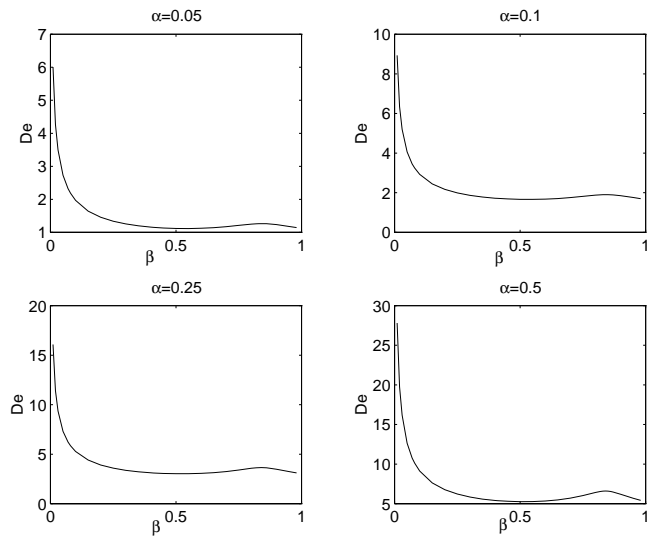


Figure 8: The critical De vs. β for aspect ratios $\alpha = 0.05, 0.1, 0.25, 0.5$.

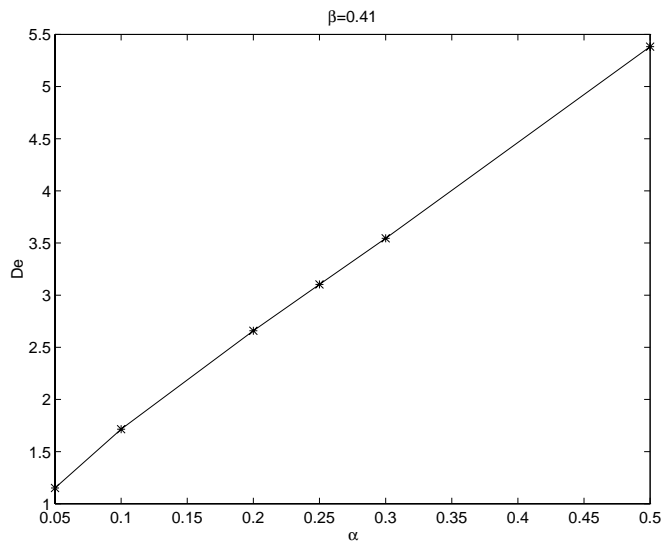


Figure 9: The critical De vs. aspect ratio α for $\beta = 0.41$.